NEXT GENERATION VEHICLE – ENGINEERING GUIDELINES FOR STAINLESS STEEL IN AUTOMOTIVE APPLICATIONS

S. Schuberth[1], E. Schedin[2], T. Fröhlich[3], E. Ratte[1]

[1]ThyssenKrupp Nirosta GmbH, Germany, [2]Outokumpu Stainless AB, Sweden, [3]ArcelorMittal Stainless Europe, France

Abstract

The objectives of the NGV (Next Generation Vehicle) Project were to demonstrate that stainless steel can be used to reduce weight and costs, and to improve safety and sustainability in structural automotive systems. The deliverables include enabling technologies, virtual technology for design and development, processing and testing. The compilation of the results as well as aspects such as new design criteria for the application of stainless steels in automotive components were arranged in an Engineering Guideline for car manufacturers and their suppliers. The program was approved by constructing several newly designed B-pillars where the deliverables were successfully applied. After performing some regular crash tests the cost efficiency was estimated by the NGV cost model. The NGV Project deliverables and data base establish a sound basis for the use of stainless steels in automotive series production.

Introduction

The automotive industry of today is characterized by faster cycles in materials invention, development and application, coupled with the ability to tailor materials for specific end-users requirements i.e. multi material solutions. It is therefore essential for materials development to be closely integrated with the final product and process concurrent engineering practice. This means being aware of

- the market and customers,
- industrial and environmental trends and forces,
- recycling,
- cost efficiency,
- and technology development.

The aim of the project is to point out to the automotive industry that stainless steel can be used to reduce weight and cost in the manufacture of motor vehicles and to improve safety and sustainability in automotive body structures. The competiveness of stainless steels should be approved in the same process steps which a standard automotive development follows: the virtual development supported by FE-simulations, the analysis of forming, tooling, joining and determination of surface and corrosion properties. These different areas mark the structure of the NGV Project. The material choice for the project and the main results of the different research areas are explained in the following.
Because of the complexity of the topic and the large experimental effort the project was organised by the three stainless steel producers ThyssenKrupp Nirosta GmbH , ArcelorMittal Stainless and Outokumpu Oyj. The European car manufacturers were represented by AUDI AG,

BMW AG, Daimler AG, Saab Automobile AB, Volvo Cars and the Centro Ricerche Fiat. For the different working groups experts were integrated to ensure that the experiments conducted are according to the current state of the art.

Material

Traditionally, stainless steels are classified mainly by their microstructure. The major basic groups are martensitic, ferritic, austenitic and duplex (austenitic & ferritic) materials. The area of use for stainless steels is very vast and comprises mainly applications taking advantage of properties such as resistance against corrosion and/or very high or low temperatures as well as hygienic surfaces and aesthetic appearance. Increasingly, stainless steels are being used also for their mechanical properties such as the combination of very high strength and excellent formability together with high energy absorption capability in finished components. The stainless steels used in the NGV Project are all but one austenitic and that one is duplex, Table 1. The chemical composition of the different grades is given in Table 2.

Table 1. Material selection for the NGV Project

EN	Type	Finishing	Supplier
1.4376	Austenitic	2B[1]	ThyssenKrupp Nirosta (TKN) ArcelorMittal Stainless Europe (AMSE) Outokumpu (OS)
1.4318 1.4318 C1000	Austenitic	2B[1] Temper C1000[2]	
1.4310 1.4310 C1000	Austenitic	2B[1] Temper C1000[1]	
1.4162	Duplex	2E[3]	

[1] Cold rolled, annealed to retrieve material properties after cold rolling, pickled and skin passed
[2] Reduced by cold rolling and achieved desired mechanical properties maintained, C1000 stating the tensile strength
[3] Cold rolled, heat treated, mechanically descaled and pickled

Table 2. Chemical composition of materials investigated

Grade	C	N	Cr	Ni	Mo	Mn
1.4376	0.03	0.19	17.6	4.2	0.15	6.5
1.4318	0.025	0.11	17.5	6.6	0.20	<1.3
1.4310	0.10	0.03	17.0	7.0	<0.6	<2.0
1.4162	0.03	0.22	21.5	1.5	0.30	5.0

The austenitic materials referred to in these Guide Lines have mostly a more or less pronounced unique feature and that is deformation- or strain-induced hardening through a forming of martensite in the material. Thus facilitating cold rolling to very high strength levels or creating strength during forming operations.

Mechanical properties

Tensile tests on stainless steels are done according to EN 10002 standard, i.e. specimen geometry and preparation, test conditions (position relatively to the rolling direction, temperature indicated, etc). Tests are typically performed at room temperature (296 K), on as-received material in the three directions (0°, 90° and 45°). The mechanical properties and r-values are summarized in Table 3. The n-value is generally determined according to the standard above mentioned; computed between 18-40% for annealed grades and between 5-17% for temper rolled C1000 grades. Even if n-values are available, they are not very meaningful when

considering austenitic stainless steels prone to deformation martensite formation since they do not describe the complete curve. Figure 1 shows such an example in the case of 1.4318 where the Hollomon model cannot fit the tensile curve because of two slopes due to the TRIP effect.

Table 3. Mechanical Properties (non-isothermal test conditions)

Value (unit)	1.4376	1.4318	1.4318 C1000	1.4310	1.4310 C1000	1.4162
$Rp_{0.2}$ (MPa)	410	420	800	300	950	600
Rm (MPa)	740	765	1050	800	1050	840
A80 (%)	40	35	18	45	25	30
R_0	0,83	0,89	0,61	0,97	0,97	0.68
R_{45}	0,96	0,98	0,62	0,97	0,97	0.65
R_{90}	0,88	0,92	0,80	0,96	0,96	0.82

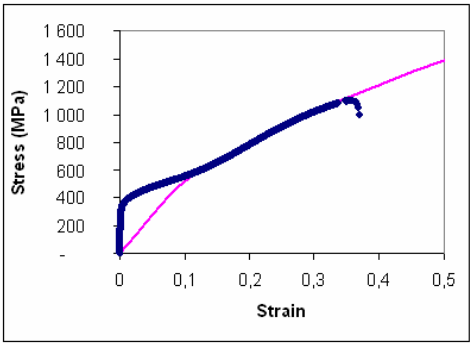

Figure 1. Comparison between the Hollomon model and the tensile curve for 1.4318

The materials here described are however not only prone to hardening through phase transformation but the rate of transformation is also dependent on strain rate as well as temperature. Consequently data from different temperature histories are of importance for forming simulation and for softwares to be able to handle those parameters. Additional to the standard tensile testing non-isothermal tests and isothermal tensile tests were conducted to determine the parameters necessary to fit the models describing the martensite formation. Additional to the quasistatic tensile tests, dynamic material properties were investigated according to the PUD-S (Prüf- und Dokumentationsrichtlinie now SEP 1240 [3]). The dynamic material properties are measured in high speed tension tests at 1, 10, 100 and 250 s^{-1}.
For a complete material description in FE-simulation the knowledge about a suitable failure criteria is necessary. The most common experimental technique is the Nakajima method. Test specimens and conditions follow generally the PUD-S. Some differences or adaptations particular for stainless steels can occur in specimen geometry (not parallel length for sample) stamp diameters (100mm is standard for thick and temper 50 or 75 mm can be used) or in multilayer lubrification system.
The material properties are completed by fatigue tests. Wöhler curves (high cycle fatigue data), Manson-Coffin curves (low cycle fatigue) and cyclic hardening data are available on some NGV grades.

Simulation

Development of Input-data

The occurring TRIP-effect has a great impact of the forming behaviour and the resulting strength. Consequently the material models which are implemented into the FE-code have to consider the martensite formation and the resulting hardening. Additionally, it needs to provide a forming history containing information about the resulting strength distribution and thereby facilitating a correct base for crash simulation.
Two different material models, both considering the TRIP-effect and its temperature sensitivity, have been used for the project. The first model is the Hänsel-Model [1]. For the implementation two minor additions were made which avoid on the one hand that the hardening modulus will approach infinity as the plastic strain reaches zero and on the other hand the initially used yield surface according to von Mises was replaced by that of Barlat and Lian. The second model used

is the Guimares model [2]. One major difference between the models is the different number of parameters which is 13 for the Hänsel model and 4 for the Guimares model. The resulting material behaviour was implemented with a simple mix-law.
The failure prediction in FE-simulations is usually done by comparing the strain distribution in critical areas with experimental FLC. Following the discussion above the best would be to use a range of FLC, determined at different temperatures. Until such data are available or a better solution exists, i.e. the numerical determination of forming limits, it is recommended to use the FLC at room temperature as the best approximation.
After the validation of the above mentioned input-data (Figure 2 shows a deep drawn component with calculated martensite fraction), a B-pillar reinforcement was simulated using the modified Hänsel model. The crash simulation was validated with two different components: a rectangular tube was crashed in compression comparable to those crash boxes which are placed behind the bumper of a car. The second validation was done with a 3-point bending geometry (Figure 3) which was chosen because it has the same crash mode as a B-pillar which is bending. Both tests were simulated and compared to the experimental results. The prediction of forces could be improved by using the modified Hänsel model in forming and crash simulation [1].

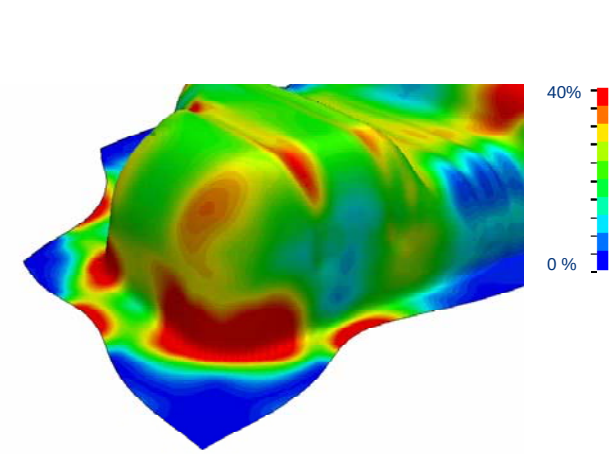

Figure 2. Simulated martensite volume

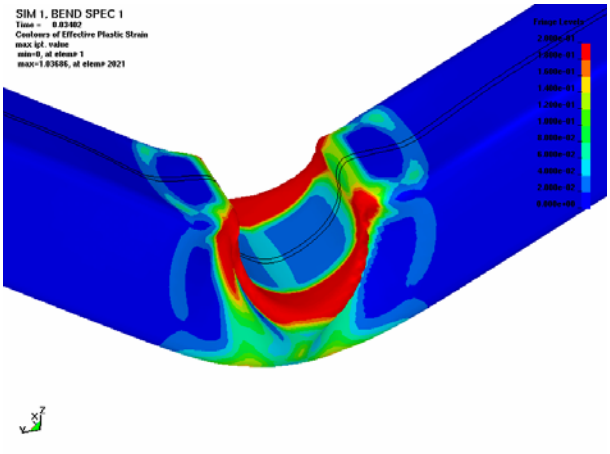

Figure 3. Simulated 3-point bending sample

Tooling

Stainless steels can in general be formed and worked by conventional processes. It is however important to remember the work hardening effects during processing which result in similar recommendations as those for high strength carbon or multiphase steels. These are of course the consideration of the higher punch- and blankholder-forces, necessary modifications of the draw bead restraining force, the use of more efficient tool material and coatings especially in critical areas as well as an optimized lubrication.
In the experiments for piercing and trimming the stainless steels 1.4376 and 1.4318 C1000 were compared. The used tool material was X70CrMoV5-2 (“Caldie”). Three different coatings, TiAlN, AlCrN, TiC were compared. Coatings were approved when at least 100.000 holes can be pierced without any burr height exceeding 60 µm and without any fatigue cracks or chipping tendencies present in the punches. For the TiC and TiAlN coatings the burr height when piercing 1.4376 is 25 µm in average. The punch force amounts to 30 N, the punch work increased during the test from around 18 J up to 20 J. Only in spalling differences between the two coatings could be observed. TiAlN did not show any signs of spalling whereas TiC showed spalling at the punch edges. Figure 4 shows the piercings at the beginning and after 100.000 strokes. Additionally, the punches after 100.000 strokes are depicted. These results show that it exists combinations of tool material/tool coating/lubricant that enable to pierce and trim stainless TRIP steels grades (fulfilling the demands from the automotive industry).

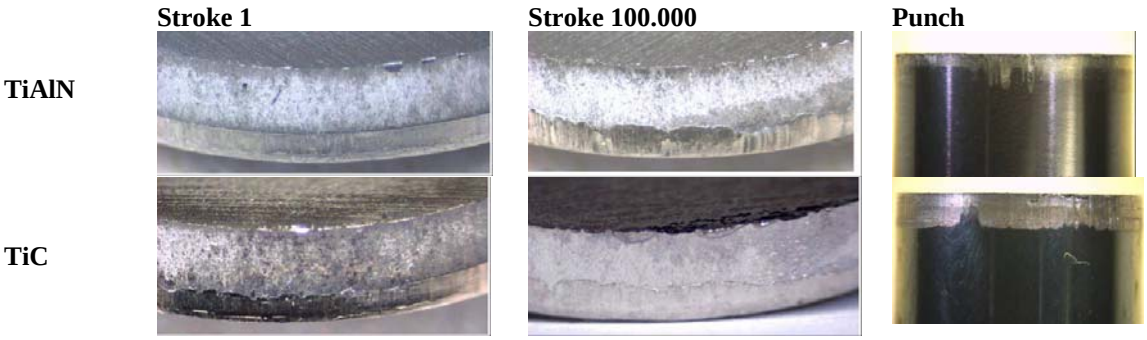

Figure 4. Comparison of piercings at the beginning and after 100.000 strokes

Joining

Stainless steels can be joined to each other as well as other materials with most common joining methods. To some extent deviations in parameters compared to what is common for mild carbon steels are inevitable. Main issue about joining stainless steels are the different physical properties compared to carbon steels that lead to different parameters compared to other steels or alloys (Table 4). Beside stainless-stainless combinations, emphasis was laid on the exploration of mixed combinations.

Table 4. Physical properties of stainless steels and other alloys

Grade	Thermal conductivity at 20°C W* m -1 * K -1	Spec. electrical resistance at 20°C Ω * mm² /m	Thermal expansion in 10-6 K-1between 20°C and 100°C
DC03 (ferritic deep drawing C-steel) DX54D (ferritic deep drawing C-steel)	50	0,22	12,0
1.4310 1.4376	15	0,73	16,0
Ecodal 6181 (AlMgSi 0.8 alloy)	≥ 190	0,033	23,4

Altogether five different processes were covered experimentally. These were resistance spot welding for stainless-stainless and mixed combinations in two and three sheet joining, resistance spot welding with an additional adhesive bonding, laser welding, MAG-welding, and adhesive bonding. After joining, the different combinations were tested in cyclic tests, the bonded samples in shear and peel-tests. Welded joints were additionally tested in corrosive environments which will be discussed in the next chapter. Due to the large experimental part, only some exemplary results can be depicted in this manuscript.
Figure 5 shows the results for fatigue testing of spot welded and spot welded samples with additional bonding. The adhesive used is Betamate 1496, which is a one component, epoxy based adhesive manufactured by Dow Automotive. The additional bonding leads to a large rise in the measured loads amplitudes, both, for stainless-stainless joints and for the mixed joint of 1.4376-DC03+ZE. The same tendency could be observed for the other combinations investigated.

Resistance spot welding

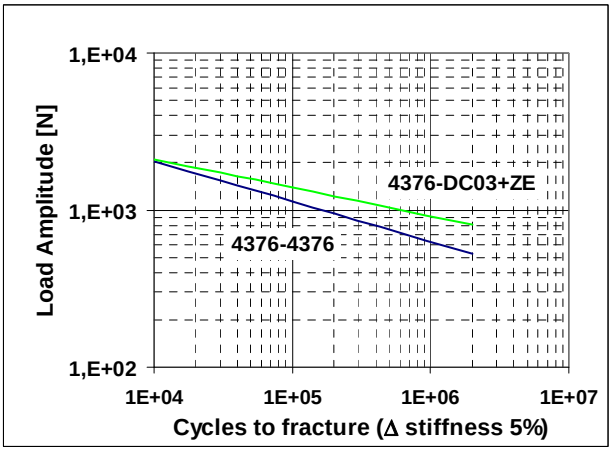

Resistance spot welding + bonding

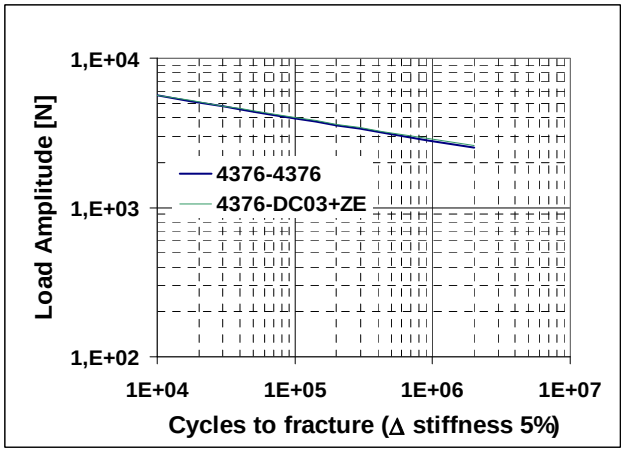

Figure 5. Comparison of fatigue tests of spot welded and spot welded + bonded samples Graph for 50% -Break down probaility, R=0,1 / f=90 Hz / T=25°C

Tailor welded blanking is an interesting method for optimizing components in regards of function as well as weight. Stainless steel can readily be used for that purpose in combination with other stainless steels or even with carbon steels which works with very good results as can be seen in Figure 6. Important factors to consider in laser welding are the laser power, the welding speed, the intensity of allocation, the focus diameter, the edge quality and positioning and the gas distribution.

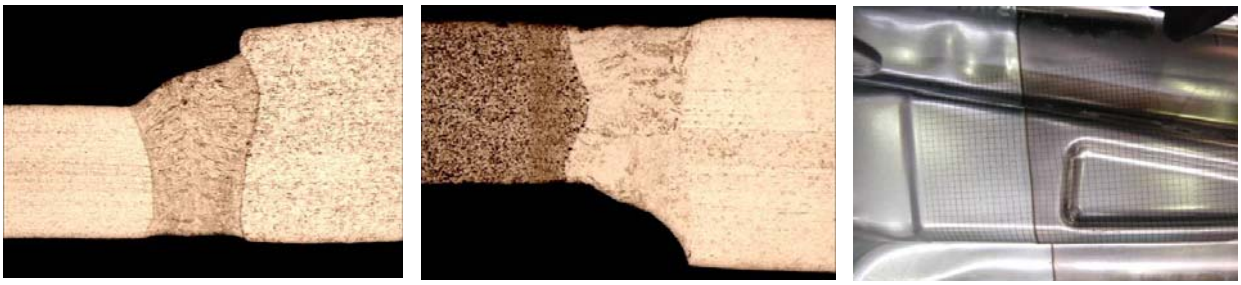

H400-H400 ***HXT600X+Z-1.4318c*** ***1.4318C1000 - DP600ZE***

Figure 6. Microcraphs of stainless-stainless and mixed laser weld, tailor welded blank

The most significant overall statements of the joining investigations were that stainless steels are weldable to each other and in mixed material joints. When employing resistance spot welding a higher electrode force might be necessary. MAG welding is suitable as well, but as for coated carbon steels, joints of stainless and coated carbon steels may show porosities. In laser-welding attention should be paid to the clampings and evaporation of zinc in dissimilar joints. The bonded joints show good values in shear and peel test.

Surface and Corrosion

Due to the passive layer stainless steels are resistant to humid atmosphere and to pure water, keep a bright shiny and stainless surface, and do not show rust as unalloyed steels and iron do. Generally, corrosion does only occur in very aggressive media (strong acids or hot strong alkalis) where the surface oxide film is not stable anymore. More relevant for daily life applications are forms of localized corrosion such as pitting and crevice corrosion. Stress corrosion cracking which can develop under very specific conditions included the effect of media bearing chloride ions. Consequently, the surface and corrosion part will primarily deal with forms of localized corrosion which may become relevant for automotive applications of stainless steels. In addition,

strategies for avoiding galvanic corrosion when pairing stainless steels with less noble materials are discussed.
Especially after resistance spot welding the joint may be affected by localized corrosion and stress corrosion cracking. To avoid corrosion of the joints the seam can be protected by wax, by coatings which provide a cathodic protection, or in case of the spot welds with adhesive bonding by the adhesive, Figure 7.

RSW RSW+Bonding RSW+Bonding

Figure 7. RSW not protected with rust formation, and RSW which are protected by the bonding after salt spray test

Implementation of knowledge gained in B-pillar concepts

One major aim of the project was to transfer the knowledge gained as fast as possible to a new product development. Therefore each car manufacturer developed a B-pillar design as a mixed material concept. The concepts differed in terms of material choice, forming procedure and joining techniques, Table 5.

All of the concepts investigated lead to a decrease of weight compared to the reference concept which is fully made of carbon and multiphase steel. To check the cost efficiency of the newly developed concepts a calculation of costs was done. Based on the parameters of the ULSAB-study a calculation tool was developed which allows a closer view on the costs of the different processes, materials and joining techniques. Assuming that the maximum scrap volume does not exceed 40% of the initial blank size, concept C and E without otimization come already close to the reference concept.

Table 5. B-Pillar concepts of the NGV project not optimized

B-Pillar	**Reference**	**C**	**E**
Material	Rephos DP600	Rephos 1.4310-C 1000 + DP 600	Rephos 1.4310-C 1000 + DP600
Process	Tailor weld	Tailor weld	Rollform
Δ Wght	**-**	- 3.51 kg	- 4.81 kg
Δ Cost/ Δ Wght		4,40 €	0,40 €

To compile the results from the different work packages, two B-pillars (concept Hydroforming and Concept Stamping with tailor welded blanks) were on the one hand virtually designed which includes the forming simulation of e.g. the hydroformed parts, the mapping of results for the crash simulation and the crash simulation itself (Figure 8). On the other hand they were produced and crash-tested. A comparison of acceleration as function of time showed a good matching of the calculated level with the experimental results. The analysis of the maximum displacement reveiled, that the simulation underestimates the intrusion which might be due to a overestimation of calculated strength. Nevertheless, the results show that a continuous simulation is possible and already comes to reasonable results. In the future the underlying models should be further adapted to optimise the simulated results.

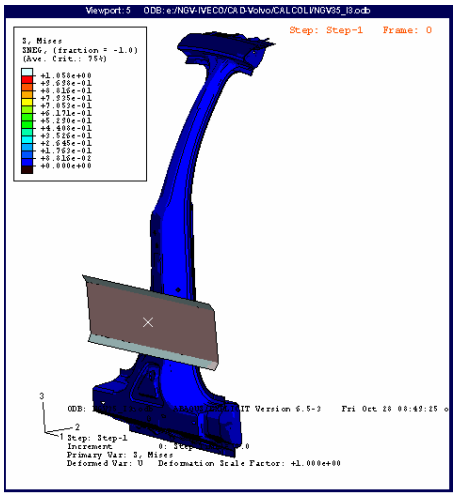

Figure 8. Model for crash-simulation

Figure 9. B-pillar for experimental crash-test

Conclusions

- Stainless steels show very good combinations of strength and ductility which is of special interest in automotive applications. The use of this materials presuppose the safe and correct use in all stages automotive development and production.
- In virtual development, the description of the material behaviour could be improved by the implementation of temperature sensitive models which allow the prediction of martensite and thus a more accurate strength determination in the virtual modelling.
- In tooling and forming stainless steels show the same restrictions as high-strength carbon steels do. Coatings such as TiAlN withstand the high forces and allow an accurate forming.
- Joining of stainless steels in uni-material and mixed joints is possible. In some cases deviations in parameters compared to what is common for mild carbon steels are inevitable but in general not greater than for different grades of carbon steel.
- To avoid corrosion of the joints the seam can be protected by wax, by coatings which provide a cathodic protection, or in case of the spot welds with adhesive bonding by the adhesive to ensure a continuity of the corrosion resistance.
- The implementation of the results into the design of several B-pillar concepts shows on the one hand the potentials for a further weight reduction and on the other hand the cost efficiency of some concepts. Designing with stainless steel need not necessarily to be adversarial compared to mild and multiphase steels especially in terms of weight savings and by the same time reasonable costs.

References

[1] A.H.C. Hänsel, P. Hora, and J. Reissner, “Model for the kinetics of strain-induced martensitic phase transformation at non-isothermal conditions for the simulation of sheet metal forming processes with metastable austenitic steels”, Simulation of Materials Processing: Theory, Methods, and Applications, Huétink and Baaijens (eds), Balkema, Rotterdam ,1998

[2] P.-O. Santacreu, J.C. Glez, N. Roulet, T. Fröhlich, Y. Grosbety, “Austenitic Stainless Steels For Automotive Structural Parts”, SAE papers 2006-01-1215

[3] Stahl-Eisen-Prüfblatt (SEP) 1240: “Prüf- und Dokumentationsrichtlinie für die experimentelle Ermittlung mechanischer Kennwerte von Feinblechen aus Stahl für die CAE-Berechnung”.